



Estimation of the Mechanical Properties of Poly(3-hydroxybutyrate) from IR Data

Péter Polyák^{1,2} · Fruzsina Mackei^{1,2} · Ágoston Tóth^{1,2} · Márton Bredács³

Accepted: 16 May 2023 / Published online: 13 June 2023
© The Author(s) 2023

Abstract

Despite the sustainability, biodegradability, and biocompatibility of microbial polyesters, as well as their potential to replace polyolefins, the market share of these biopolymers is still marginal. The primary factors that impede the success of microbial polyesters are related to their poor thermal stability and the degradation during processing that negatively affects the mechanical performance of the final product. Due to the complexity of the mechanism of degradation and the vast number of factors that influence the mechanism, the outcome of the degradation cannot be predicted with high confidence. Our present work addresses both difficulties. First, the thermal stability of poly(3-hydroxybutyrate) was successfully improved by a stabilizer system based on pomegranate extract. Second, we have developed a computational method that can be used for the estimation of the mechanical properties of processed microbial polyesters from IR data. The computational method is based on an unprecedented hybrid model that incorporates both linear and nonlinear components. The linear component is based on multivariate data analysis and quantizes the correlation between IR data and the extent of degradation. In contrast, the second component consists of a power function in order to be able to describe the nonlinear correlation between the extent of degradation and the mechanical properties. By using the hybrid model, indicators of mechanical performance, such as tensile strength, can be estimated from IR data, which was not achieved before.

Keywords PHB · Microbial polyester · Degradation · Stabilizer · PCR · PLS

Introduction

Although the future prospects of the polymer industry are subject to intense debate, the vast majority of researchers agree that goals such as sustainability and independence from fossil resources are of equal importance. Moreover, the lifecycle of polymers must also be completely circular, i.e., the metabolites of the degradation should be used as a

feedstock for the synthesis of new polymers. Biopolymers, for instance, meet these requirements. According to the definition of IUPAC, biopolymers are macromolecules formed by living organisms; i.e., an artificially synthesized polymer cannot be regarded as a biopolymer. Microbial polyesters satisfy all criteria related to sustainability and recyclability and are also considered biopolymers as per IUPAC definition, since they are natively synthesized by bacterial strains that utilize them as intracellular material and energy storage. Microbial polyesters are fermented using various carbohydrates [1–3] and lipids [4, 5] originating from plants. To improve the efficiency of production, several research projects were carried out over the past few decades that targeted the fermentation of microbial polyesters using waste materials. These sources include agricultural waste [6], kitchen waste [7], or even wastewater [8].

The first material source (carbohydrates) is produced in vast quantities by photosynthesis in the biosphere, amounting to approximately 220 billion metric tons per year [9]. As long as photosynthesis occurs on Earth, this material source cannot technically be depleted. Similarly, the materials

✉ Péter Polyák
polyak.peter@vbk.bme.hu

¹ Laboratory of Plastics and Rubber Technology, Department of Physical Chemistry and Materials Science, Budapest University of Technology and Economics, Műegyetem Rkp. 3., 1111 Budapest, Hungary

² Institute of Materials and Environmental Chemistry, Research Centre for Natural Sciences, ELKH Eötvös Lóránd Research Network, Magyar Tudósok Körútja 2., 1117 Budapest, Hungary

³ Polymer Competence Center Leoben GmbH, Rosegger Street 12, 8700 Leoben, Austria

belonging to the second category (lipids) are available in the form of plant oils [4, 5, 10]. The produced volume of these materials has already been scaled up due to the high demand for biodiesel, which is heavily dependent on the availability of plant oils [11, 12]. Recent reports have also proven that even the side-product of the biodiesel industry, *e.g.*, glycerol, can be a feedstock for polyester production [13]. The third source of materials for the fermentation of microbial polyesters (agricultural waste) is also abundant. For instance, the extraction of carbohydrates from plants also yields vast amounts of lignin as a byproduct. Currently, most of this byproduct is used in a rather rudimentary way: lignin is burned in order to salvage at least some energy. However, Herrera and his coworkers reported that lignin could also be used as a substrate for the fermentation of microbial polyesters [14].

These findings clearly show that the substitution of conventional polymers with microbial polyesters could shift the polymer industry towards a sustainable model. Unlike several of their competitors (*e.g.*, polyolefins), microbial polyesters can be degraded and completely decomposed hydrolytically [15]. Although their depolymerization in a strong alkali or acidic medium is technically feasible, there are more sophisticated methodologies. For example, the depolymerization of microbial polyesters might be catalyzed enzymatically [16, 17]. Enzymes generally prefer mild conditions: neutral or near-neutral pH and temperatures close to room temperature. Therefore, enzyme-catalyzed degradation of microbial polyesters could also be a significant step towards a green and sustainable polymer industry.

Although the list of beneficial features of microbial polyesters presented and discussed above is quite extensive, there are a number of disadvantages as well. For example, the replacement of conventional polymers with microbial polyesters in the packaging industry faces two obstacles. The first one is their price: despite the efforts that target the fermentation of these biopolymers using inexpensive material sources [1–3], their price is still higher than that of their competitors, *e.g.*, polyolefins. The second one concerns the processing of microbial polyesters: technologies of high throughput, *e.g.*, injection molding or extrusion, process the polymer in the melt. Consequently, heating the material above its melting temperature (T_m) is inevitable. Unfortunately, above their T_m , neat microbial polyesters tend to degrade rapidly.

The first difficulty outlined above is addressed by several research projects that target their fermentation using cheap substrates [18–22]. As a result, the price of microbial polyesters was reduced to the range of \$4–6/kg (*i.e.*, five to six times that of polyolefins) and is expected to decrease even further [23]. Since the stabilization of microbial polyesters has not been extensively studied yet, the second challenge appears to be formidable. There are, however, a handful of publications dedicated to the investigation of the degradation

of microbial polyesters [24, 25]. Santos *et al.* studied the thermal degradation of microbial polyesters [24], while Michalak attempted to provide a detailed and comprehensive description of the thermo-oxidative degradation of these macromolecules [25]. Although the mechanism was reported to be highly complex and many questions were left unanswered, there are a few characteristics of the thermo-oxidative degradation of microbial polyesters that are certain. One of the most important ones is the dominant degradation mechanism, which is statistical chain fragmentation [25].

Statistical chain fragmentation must be impeded; otherwise, the process deteriorates mechanical performance considerably. For this purpose, stabilizers may be used. Due to their importance in the polymer industry, stabilizers are very intensively studied and thoroughly characterized [26–28]. However, the vast majority of conventional stabilizers are artificially synthesized compounds that are derived from fossil material sources. In order to create a completely sustainable polymer industry, natural materials should be preferred over those produced by traditional synthetic methods. Fortunately, stabilizers of purely natural origins have drawn attention in the past few years. As a result, several articles are already available in the corresponding literature that discuss the utilization of bio-based materials as stabilizers of polymers [29–31].

Although bio-based stabilizers undoubtedly contribute to a more sustainable polymer industry, these additives inevitably have a number of drawbacks as well. For example, natural stabilizers are often available as plant extracts [32, 33], which typically comprise a mixture of various compounds. In addition, the composition of plant tissues heavily depends on many factors that cannot be controlled directly, such as the amount of rainfall, sunshine, type of soil, and so on. Consequently, the relative quantity of components in plant extracts is known to vary from batch to batch. This variation and unpredictability could potentially hinder the introduction of plant extracts as stabilizers of microbial polyesters to the market.

To overcome these difficulties, a method is proposed that facilitates the estimation and prediction of mechanical properties of microbial polyesters that contain natural stabilizers. Our concept is based on the analysis of the IR spectra of the stabilized polymer. The thermo-oxidative degradation of polyesters is known to alter the IR spectra of the samples considerably [34, 35]. The changes caused by the degradation are difficult to attribute to individual reactions due to the remarkable complexity of the parallel and consecutive subtractions [25]. However, the mathematical tools offered by principal component regression (PCR) [36] and partial least squares method (PLS) [37] enable us to identify and quantitatively characterize the correlation between independent and dependent variables, even if the former is represented by large datasets, *e.g.*, thousands of absorbance values in

the IR spectra. PCR and PLS are already extensively used in several scientific fields, such as agricultural [38–40], protein [41, 42], and pharmaceutical [43] sciences. Although these methods have started to become more widely used in the polymer industry as well [44], their applications remain limited. For instance, the goal of our study, i.e., the estimation of mechanical properties of processed microbial polyesters from IR data, was not achieved before.

Experimental

Preparation of the Samples and Their Degradation

First, poly(3-hydroxybutyrate) PHB (Metabolix Mirel M2100) was dried (70 °C, overnight) to avoid hydrolytic degradation of the polyester. After drying, solvent-cast films and compression-molded plates were created. The manufacturing of both types of samples started with the dissolution of the polymer in chloroform (Molar Chemicals Ltd.); the concentration of the polymer was 3 m/m%. The dissolution was carried out in a stirred round-bottom flask (300 RPM) at the boiling point of the solution (approximately 65 °C) and lasted 2 h. Once the flask cooled down to room temperature, the components of the stabilizer system were added to the solution.

The primary stabilizer was pomegranate extract; as the secondary stabilizer, PepQ (Clariant AG) was selected. The source of the primary stabilizer was powdered pomegranate peel (Turkey); the material was obtained by Soxhlet extraction with acetone. The targeted extracts were recovered from acetone in a rotary evaporator. Both stabilizers were added to the solution of the polymer in a concentration of 0.1 m/m% with respect to the polymer. The last component was the IR internal standard; for this purpose, polydimethylsiloxane (PDMSO) was used. PDMSO was used in a concentration of 4 m/m% with respect to the mass of PHB. Subsequently, the solution was homogenized (room temperature, 300 RPM, 1 h), and the insoluble components of the pomegranate extract were removed.

From the purified solution, 7 cm x 7 cm films were created by solvent-casting; their average thickness was measured to be ~35 µm. These films were used in degradation studies ‘as is’ and also served as a starting material for the fabrication of compression-molded plates. First, six films were cast, stacked on top of each other, and placed into a 7 cm x 7 cm metal frame of 200 µm thickness. The sample was compression molded in a custom-made laboratory press pre-heated to 180 °C, with a pressure of 20 kN. Under these conditions, approximately 1 min was found to be sufficient for the formation of a homogeneous plate.

Two types of degradation studies were conducted. The first sequence of measurements was carried out using the

aforementioned laboratory press, whereas the second sequence was performed in a heating oven. While selecting the parameters of degradation, our aim was to simulate the conditions that are typical for conventional processing technologies such as injection molding or extrusion. Therefore, the atmosphere was oxidative (air), and the temperature was set to 180 °C. The time of degradation ranged from 1 to 12 min with an increment of 1 min. Thus, 12 degradation times were selected (1, 2, 3, ..., 12 min) in addition to the undegraded samples. In each case, three samples were investigated, i.e., three parallel measurements were carried out per degradation time per degradation method.

Analysis of the Degraded Samples

Mechanical properties were characterized by tensile testing. Solvent cast films were analyzed with an Instron 34SC-05 machine (equipped with a 100 N cell), whereas compression molded plates were tested with a Zwick/Roell 1445 instrument (equipped with a 1000 N cell). From each 7 cm x 7 cm sample, three dumbbell-shaped specimens were cut that had a width of 4 mm in the middle. Solvent-cast films and compression molded plates had an approximate thickness of 35 µm and 200 µm, respectively. Precise values were determined with a micrometer prior to the tensile test. Each measurement was carried out at 5 mm/min crosshead velocity and 40 mm gauge length.

Spectral data was collected with a Bruker Tensor 27 IR spectrophotometer equipped with an ATR accessory. The spectrum of each sample was recorded five times between 400 and 4000 cm^{-1} with 1 cm^{-1} resolution; the measurements consisted of 16 scans. As a first step of spectral pretreatment, manual baseline correction was carried out. Absorbance values at 4000, 3750, 3500, 3250, 2750, 2500, 2250, 2000, 1500, and 400 cm^{-1} were extracted. At these values, neither the polymer nor any of the additives have an absorbance. The absorbance values at the wavenumbers listed above were plotted, and a 3rd-order polynomial was fit onto the points with a nonlinear iterative algorithm (Levenberg–Marquardt). Then, the value of the polynomial was calculated at each investigated wavenumber between 4000 and 400 cm^{-1} and subsequently subtracted from the corresponding empirically collected absorbance value. This way, the modified absorbance values became equal to or approached zero in wavenumber regions where none of the components of the sample absorbed photons.

As a next step of the pretreatment, the amplitude of the spectra was adjusted. The internal standard (DMSO) is completely inert; therefore, its peaks have the same size regardless of the extent of degradation. The peak of DMSO present in the 790–820 cm^{-1} region is almost completely separated from the others. Accordingly, this peak was selected as a basis for the amplitude correction: all spectra

were multiplied by a scalar that set the maximum value of the reference peak precisely to 0.1. As a last step of the preliminary calculations, spectra belonging to the same degradation time were averaged.

Results and Discussion

The results are discussed in multiple sections. First, the principles of the model that enables the quantitative characterization of the correlation between mechanical properties and the IR spectra will be introduced. In the next section, data that empirically proves the feasibility and relevance of the modeling is presented and discussed. Then, the process of building the model is described in detail. In the final section, the model is optimized and applied in practice.

Introduction and Description of the Hybrid Model

The hybrid model consists of two parts. The first part describes the correlation between the mechanical properties and the extent of degradation. The second part is dedicated to the quantitative characterization of the correlation between the IR spectra of the polymer and the extent of degradation. To construct the first half of the model, one indicator of mechanical performance, and one indicator of the extent of degradation must be selected. The mechanical performance will be characterized by tensile strength, whereas the extent of degradation will be quantized by the time of degradation, i.e., how long the polymer was exposed to thermo-oxidative stress. This value can be very precisely and reproducibly measured; therefore, the time of degradation appears to be an optimal choice to be used as an independent variable of the first half of the model. As presented in Fig. 1, the tensile strength plotted against the time of degradation shows a clear negative correlation that may be approximated with a simple function that takes one independent variable (time of degradation) and outputs one dependent variable (tensile strength).

Although fitting a simple polynomial to the empirical points observed in Fig. 1 is completely feasible, we found that at least a third-order polynomial is required for an adequate fit. Third-order polynomials assume the introduction of four parameters. Conversely, the fit of the same quality can be achieved if a power function of only two parameters is used instead. Accordingly, in order to keep our model as simple as possible, a power function was used; see Fig. 1 and Eq. 1.

$$\sigma = A \cdot (1 + t)^B \quad (1)$$

In Eq. 1, σ denotes the tensile strength in Pascal (Pa), and t denotes the time of degradation in minutes (min).

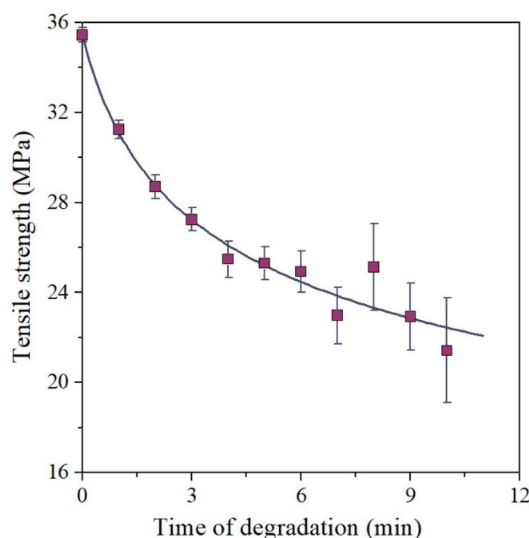


Fig. 1 The time of degradation correlates negatively with the tensile strength of the polymer

A and B are regression parameters. In the case of our samples, prepared according to the method described in the experimental section, the best fit was achieved with $A = 35.48$ and $B = -0.1909$. The R^2 value of the regression was calculated to be 0.9717, which validates that Eq. 1 can provide an acceptable approximation of the empirically obtained values, even though it contains only two regression parameters.

Figure 1 suggests that the first half of the model, i.e., the correlation between the mechanical properties of the polyester and the time of degradation, may be represented by a simple function with one dependent and one independent variable. Contrarily, the second half of the model (i.e., the correlation between the time of degradation and the shape of the IR spectra) assumes a significantly more complex mathematical apparatus. This complexity is due to the number of independent variables: IR spectra consist of thousands of individual absorbance values. Therefore, a model is to be constructed that takes thousands of values as independent variables and outputs one single dependent variable: the time of degradation.

Such models can be constructed in many ways; the most effective, reliable, and robust ones are based on the computational tools offered by multivariate data analysis. Among these tools, principal component regression (PCR) and partial least squares methods (PLS) gained popularity in recent years. Since PCR and PLS are both capable of the accurate mathematical representation of this correlation, the second half of the model will be based on PCR and PLS. In contrast with the first half of the model, both PCL and PLS are linear methods and take many independent variables. The combination of the first (nonlinear) and second (linear) halves

results in the final (hybrid) model, as presented graphically in Fig. 2.

Empirical Proof of the Feasibility of Modeling

Figure 1 demonstrates a strong negative correlation between the time of degradation and the tensile strength of PHB. Accordingly, a model equation fit to the empirical points can represent the correlation very well; see the regression curve in Fig. 1. In contrast, the possibility of modeling the relationship between the time of degradation and the shape of IR spectra may not seem obvious at first sight. The effect of degradation on the shape of the IR spectra is observable even without in-depth numerical analysis, but the mathematical description of this covariance might be challenging. Therefore, proving that there is a correlation between the time of degradation and the measured IR spectra is essential. To achieve this, the Pearson correlation coefficient was calculated at each wavenumber. This coefficient was computed between the time of degradation and the absorbance of the sample degraded for the corresponding amount of time. The

coefficients calculated in this way were plotted against their respective wavenumber; see Fig. 3.

The correlation coefficient approaches either +1 or -1, but rarely takes values in between. This tendency means that there is either a strong positive (+1) or a strong negative (-1) correlation between the time of the degradation and the absorbance at a given wavenumber. Correlation coefficients close to zero indicate little to no correlation. However, near-zero correlation coefficients were rarely calculated: the values plotted in Fig. 3 tend to approach their extrema. In practical terms, this tendency means that the ongoing degradation either increases the IR absorbance (correlation coefficient approaches +1) or decreases it (correlation coefficient approaches -1). Regions of the IR spectrum where the degradation does not shift the absorbance in any definite direction are rare and narrow.

Thus, the effect of the degradation on the measured absorbances appears to be deterministic: degradation either increase or decrease the absorbance. Wavenumber regions where degradation stochastically alters the absorbance, thereby resulting in a near-zero correlation coefficient, are sparse and limited in width. In simpler words, the effect of degradation on IR absorbances is deterministic because the increasing time of degradation either increases individual absorbances or decreases them. The former tendency, i.e., the ongoing degradation increases the absorbance, is demonstrated in Fig. 4a. The latter tendency, i.e., the longer the time of degradation, the smaller the peak becomes, is shown in Fig. 4b. As a supplementary file, a video was also prepared to animate the scatter plot changes through the investigated wavenumber range; see file S1.

Figure 4 shows that measured points do not align perfectly to a straight or curved line, i.e., they cannot be perfectly described by one single equation, such as Eq. 1. However, the positive or negative correlation is clearly observable, regardless of the wavenumber. We can conclude, therefore, that at the majority of investigated wavenumbers, there is either a positive or a negative correlation between the time

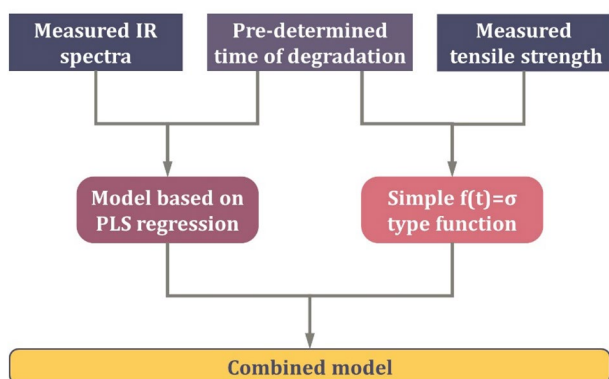
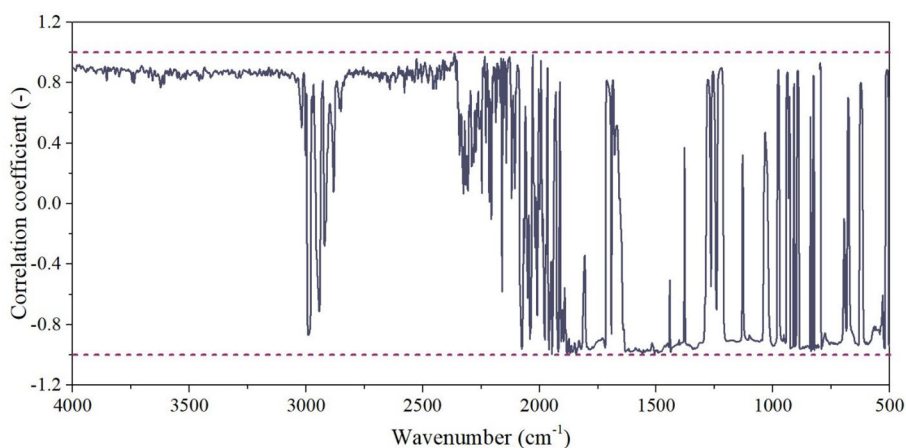


Fig. 2 Graphical representation of the method used to construct the hybrid model

Fig. 3 The correlation coefficient is in the proximity of either +1 or -1, suggesting that the impact of degradation on the absorption peaks is fully deterministic



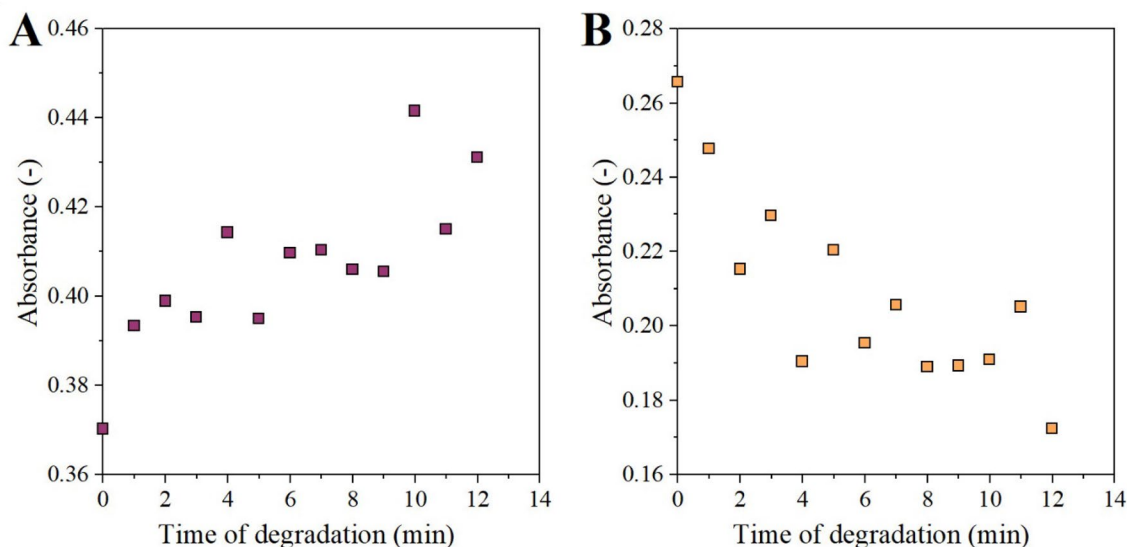


Fig. 4 Absorbances plotted against the time of degradation. At some wavenumbers, the correlation is positive (1122 cm^{-1} , to the left), while at others, the correlation is negative (1175 cm^{-1} , to the right)

of degradation and the measured absorbances. Accordingly, this correlation can be modeled and used as the second half of our hybrid model. Since the input of the model consists of thousands of individual absorbance values in this context, advanced mathematical methods, such as PCR and PLS, will be used.

Construction of the Hybrid Model

As mentioned in Sect. "Introduction and description of the hybrid model", the first half of the model is a nonlinear equation that enables the calculation of one dependent variable (tensile strength) from one independent variable (time of degradation). This part of the model is already introduced and explained; see Eq. 1. In contrast, the second half of the hybrid model must be capable of taking multiple independent variables as an input and is expected to be linear due to the linearity of both PCR and PLS. The building of the second part is significantly more complex and consists of several steps. First, a wavelength range containing absorbances that will be used later as independent variables must be selected. Technically, even an entire IR spectrum could be used. However, the majority of the IR spectrum of PHB does not contain significant quantitative data, as there are numerous ranges without any absorption peaks. Instead, regions must be found that contain the peaks altered the most by the thermo-oxidative degradation.

These regions can be localized by using a wide variety of methods. The most evident might be the attribution of individual peaks to functional groups. If the mechanism of the degradation is well known, one could predict which

peak will change and in which direction. For example, the dominant degradation mechanism of PHB is statistical chain fragmentation. Therefore, the height of peaks attributed to C–O–C vibrations is expected to decrease due to the break of ester bonds during degradation. Unfortunately, this method has little relevance in practice. First, the thermo-oxidative degradation of microbial polyesters is extremely complex [25] and consists of several parallel and consecutive reactions. Therefore, changes in the height of absorbance peaks can hardly be attributed to individual reactions. Second, the market of microbial polyesters changes constantly: new fermentation techniques yield new products of different parameters, such as the ratio of comonomers, quality of end-groups, quantity and quality of contaminations, and so on. Lastly and most importantly, microbial polyesters cannot be effectively processed without additives; at least a stabilizer is needed to address the poor thermal stability of the macromolecules. The presence of stabilizers is expected to change the reaction routes outlined in the article of Michalak [25] significantly.

The primary component of the stabilizer system we used here is pomegranate extract, which is a mixture of several components. According to the report of Ambigaipalan et al. [45], the extract contains 79 phenolic compounds, 35 tannins, 8 proanthocyanidins, and 8 anthocyanins. In contrast, Fisher et al. [46] identified only 48 compounds in pomegranate extract, which highlights that the qualitative analysis of the components is challenging. The extract that was used for the preparation of our samples was investigated in a previous study; the main component was found to be punicalagin [47]. The quantitative analysis of pomegranate

extract is similarly difficult, and yields results that vary in a broad interval. The main component, i.e., punicalagin, was reported to be present in the extract in concentrations that range from 2 to 500 mg/g [45–49]. As a part of a previous project, the pomegranate extract we used was also analyzed; the concentration of punicalagin was measured to be 79 ± 5.2 mg/g [47].

The disparity of the data submitted by independent research groups is probably due to the differences in the origin and quality of the fruit, the extraction technique, the method of qualitative and quantitative analysis, and so on. The advantage of our method is that the correlation between the IR data and the extent of degradation can be characterized even if we do not have an in-depth understanding of the qualitative and quantitative characteristics of the plant

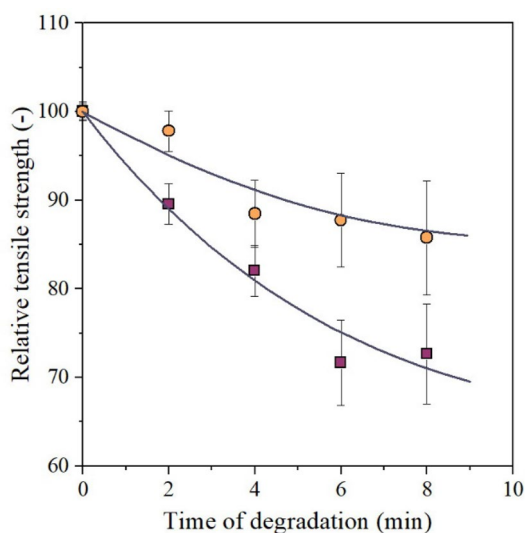
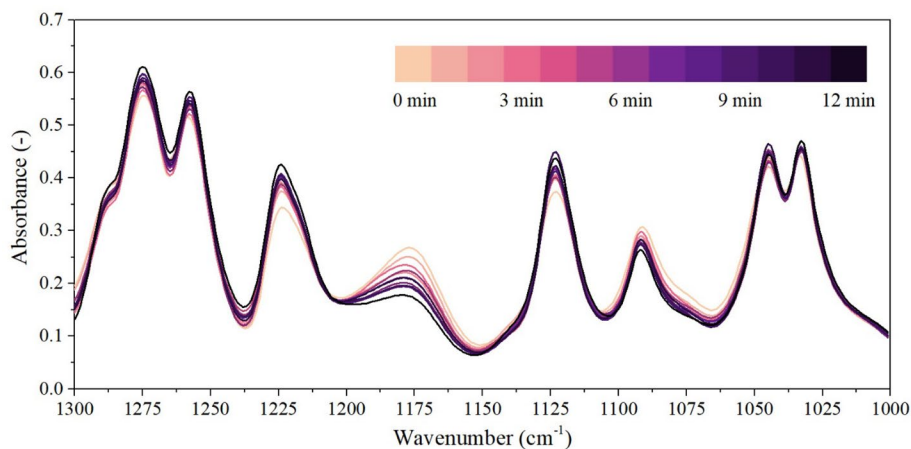


Fig. 5 A mixture of pomegranate extract and PepQ was found to effectively impede the deterioration of mechanical performance caused by thermo-oxidative degradation. Open circle: stabilized samples, open square: neat polymer

Fig. 6 Consecution of IR spectra of samples degraded for 0, 1, 2, 3, ..., 12 min

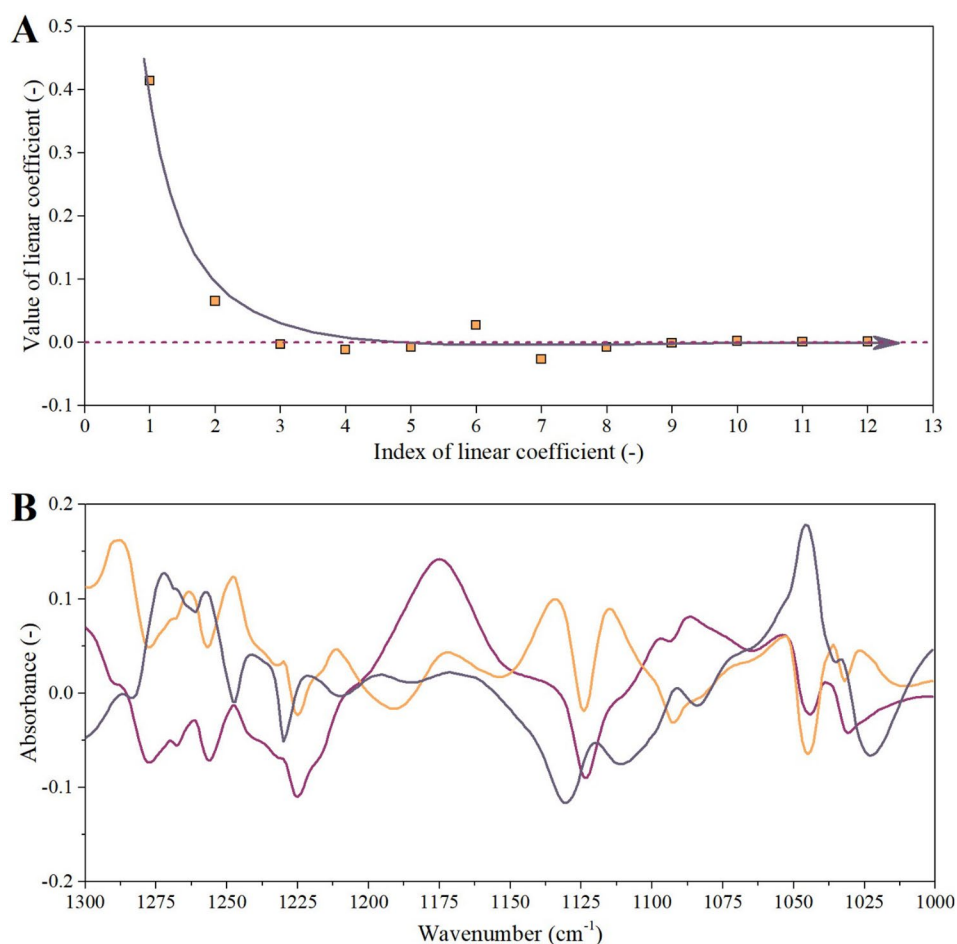


extract. Therefore, the critical parameter is the efficiency of the extract as a stabilizer, and not its chemical composition. As presented in Fig. 5, the combination of pomegranate extract and PepQ effectively slows the degradation of PHB and the resulting deterioration of mechanical performance. The difference between stabilized and neat samples proves that using natural antioxidant-based stabilizer systems is highly beneficial, even if it makes the complete qualitative analysis of the degradation nearly impossible.

Due to the vast number and complexity of the parallel and consecutive reactions, the wavenumber region the model is preferably built upon cannot be localized by searching for individual peaks altered by individual reactions. Instead, we have to look for the wavenumber regions that are altered the most by the degradation. Our preliminary studies have shown that the amplitude of peaks located in the $1300\text{--}1000\text{ cm}^{-1}$ region changed considerably during the degradation. Therefore, absorbance values belonging to wavenumbers in this region will serve as the independent variables. After the selection of the investigated range, the measured IR spectra were plotted between 1300 and 1000 cm^{-1} , as demonstrated in Fig. 6.

Although the thermo-oxidative degradation alters the absorbances in the entire investigated region, the changes are mostly subtle. Therefore, the spectra plotted above show strong linear dependence. This collinearity makes models based on direct absorbance—time of degradation regression unreliable: such models are known to be prone even to minor perturbations. The most effective way to address multicollinearity is the transformation of the data into a new Euclidean space, where most of the variance can be described with the fewest possible dimensions. The method is called principal component analysis (PCA [50]) and was performed using a software developed by our research group in MATLAB environment. Figure 7 shows that PCA is a very effective method for the reduction of dimensionality of the data plotted in Fig. 6. Most of the variance is described by the linear

Fig. 7 **a** Linear coefficients of the spectrum recorded first (i.e., $t=0$). **b**: First few basis vectors of the new Euclidean space



combination of only two principal components; see Fig. 7a. The diagram also visualizes the principal components, i.e., the basis vectors of the new Euclidean space the absorbance data was transformed into (Fig. 7b).

The IR spectra do not show collinearity in the new vector space; therefore, they can be used as the independent variables of the multidimensional linear regression that will yield the model. The combination of PCA and multidimensional linear regression is often called principal component regression (PCR [50]). We have found that PCR describes the correlation between the absorbance values and the targeted dependent variable, i.e., time of degradation accurately, even if only a few principal components are used. However, our preliminary calculations also revealed one of the weaknesses of PCR. Since PCA and multidimensional linear regression are performed independently, the calculation does not take into account the dependent variable during the computation of the principal components. This shortcoming is eliminated by the implementation of the method called ‘partial least squares’ (PLS [50, 51]). PLS was performed by a software our research team developed in MATLAB environment. The software is based on the algorithm first proposed and described here [51]. Subsequent to the completion of the

software and initial tests with both PCR and PLS, the methods were optimized and applied in practice.

Optimization and Application of the Model

The first and most important parameter of both PCR and PLS is the number of principal components they are based on. The optimal value was found as follows. Models were built by using a different number of principal components, e.g., two (Fig. 8a) or ten (Fig. 8b). Next, individual spectra belonging to different degradation times (0 min, 1 min, 2 min, ..., 12 min) were input into our software, which estimated the degradation time. The results obtained using the software that implemented the PCR method are displayed below.

Figure 8a demonstrates that the calculation predicts inaccurate results if only two principal components are used. In contrast, the model becomes overfitted if the number of principal components is increased to ten (Fig. 8b). Therefore, the optimum is to be found somewhere in between. In order to be able to determine the optimal number of principal components precisely, the accuracy of the prediction was quantized and plotted against the number of principal components that

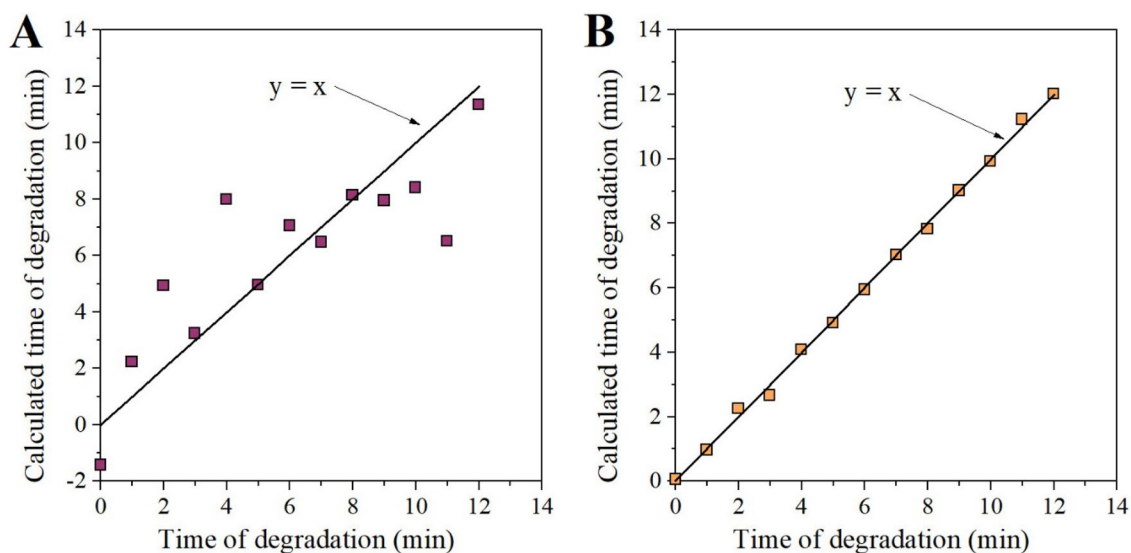


Fig. 8 Testing the accuracy of the PCR model based on two (a) and ten (b) principal components

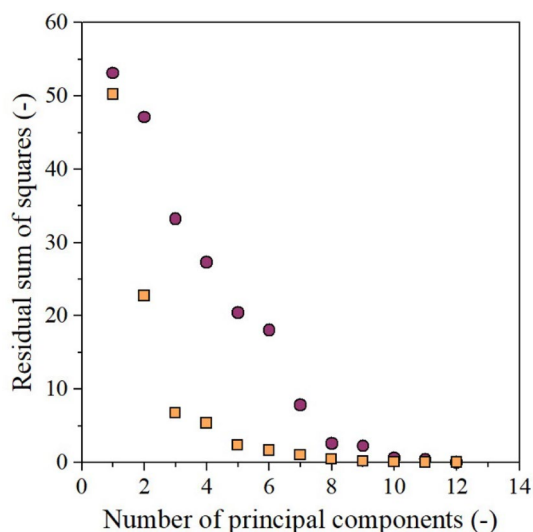


Fig. 9 Accuracy of PCR (open circle) and PLS (open square) methods as a function of the number of principal components

were used while building the model (Fig. 9). The accuracy of the prediction was quantitatively described by the residual sum of squares, i.e., the difference between actual and predicted values, squared, summed. Figure 9 simultaneously presents the number of principal components—accuracy of prediction correlation of both PCR and PLS models.

Figure 9 reveals that PLS outperforms PCR: the error of prediction calculated with PLS converges to zero faster than that calculated with PCR. Accordingly, our final model will be based on PLS. The figure shown above also helps the determination of the optimal number of principal

components. The accuracy of the prediction is increased drastically if the number of principal components is increased from 1 to 2 and from 2 to 3. However, increasing this parameter from 3 to 4 does not reduce the error function considerably. Therefore, the PLS model is based on 3 principal components.

The last and most important step of constructing any kind of computational method is its application in practice and the analysis of its reliability. The workflow of using the hybrid model is visualized in Fig. 10a. First, the IR spectrum of the sample is to be recorded. Then, the spectrum should be pre-processed with the same technique that was used during the construction of the model. This pre-processed spectrum serves as the input of the PLS method that yields one single scalar: the time of degradation. This value is to be substituted into Eq. 1; the substitution enables the calculation of the targeted yield strength.

These computational steps were also used to validate the reliability and accuracy of the hybrid model. As a first step of independent validation, an additional set of PHB samples was created and subsequently subjected to degradation that lasted 0, 1, 2, ..., 12 min. Afterward, the IR spectra and the tensile strength of the samples were measured. Lastly, the IR spectra were used as a basis for the estimation of the tensile strength, as described above and graphically represented in Fig. 10a. The estimated tensile strength values were plotted against their measured counterparts; see Fig. 10b.

Figure 10b proves that our hybrid model is capable of a rather accurate estimation of the tensile strength of PHB if the time of degradation is shorter than 6–8 min. However, at degradation times longer than 8 min, the accuracy of the model seems to deteriorate. This undesired effect could

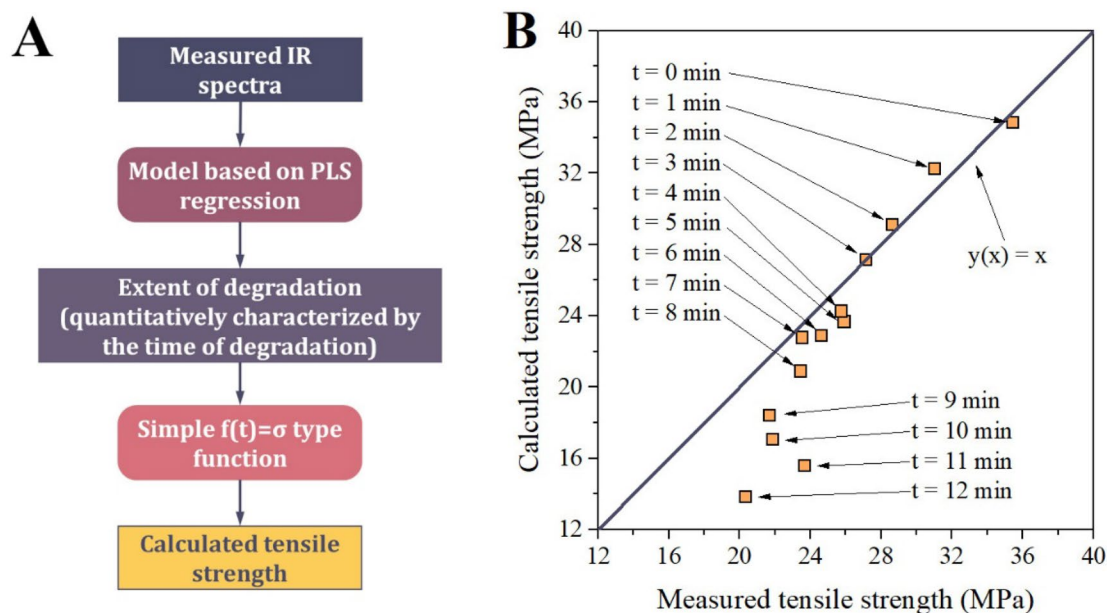


Fig. 10 Block diagram that demonstrates the workflow of using model (a) and the results of the measurements that targeted the analysis of its reliability (b)

be caused by several factors. First, the results presented in Fig. 1 indicate a positive correlation between the time of degradation and the standard deviation of the measured tensile strength values. Therefore, the prediction of tensile strength in the region where the degradation time exceeds 8 min also becomes less reliable. The second factor is related to the degradation mechanism of PHB. The results presented above have proven that the degradation of PHB is deterministic: regardless of the wavenumber, the absorbance changes in one definite direction, i.e., is either increased or decreased by the ongoing degradation; see Figs. 3 and 4. At increased degradation times, however, stochastic factors might also alter the chemical characteristics of the polyester. An important example is the formation of crosslinks; caused by the recombination of radicals. Some researchers call the process ‘gelation’. This phenomenon, observed at degradation times exceeding 8–10 min, was found to make the accurate analysis of the rheological properties of the melt very difficult. Similarly, it could also bias the analysis of IR absorbances by a stochastic error.

An additional limitation of the model is related to the mechanical shear of the melt. During processing with conventional techniques (e.g., injection molding or extrusion), mechanical shear is inevitable, and it will contribute to the degradation. In contrast, the samples used as the source of IR data were thermo-oxidatively degraded under mechanically static conditions. Therefore, the IR data does not show the effect of shear, such as the absorbance of new functional groups created by mechanical stress-induced chain fragmentation. Since this technical difficulty was encountered

by many researchers in the past, the phenomenon of shear-induced degradation has been studied extensively in the case of both neat polymers [52] and composites [53]. Due to its importance, advanced technologies, such as the finite element method (FEM), have also been applied to quantitatively describe the influence of the stress field on degradation rate [54]. An additional limitation that must be taken into consideration is related to the thermal inhomogeneity of the sample. In the case of products manufactured by any technology bearing industrial relevance, there are temperature gradients in the sample because some regions cool faster than others. Macromolecules located in regions that cool slower will be subjected to prolonged degradation. Therefore, the deterioration of mechanical performance is expected to be more significant in these areas. In order to obtain representative data, it is recommended to analyze regions where the temperature remained high for longer periods.

Despite the deviance shown in Fig. 10b and the limitations discussed above, the measurements targeting the analysis of the accuracy of the model proved that it provides reliable results in the region bearing industrial relevance. For example, the cycle time of injection molding or the residence time of extrusion are generally shorter than 8 min, i.e., the model will be used in the region where it was proven to operate with acceptable accuracy. Therefore, we would like to propose its application in practice and envision its implementation as follows. First, the polymer-stabilizer pair is to be selected. Although our measurements were carried out with PHB and pomegranate extract, the technique is not material-dependent: as long as there is a direct correlation

between the IR spectra of the material and the time of degradation, the model will prove to be functional. Therefore, different microbial polyesters and/or different stabilizers may be used.

After the selection of the materials, the two halves of the model are to be constructed. The first half mathematically represents the correlation between the tensile strength and the time of the degradation; the second half does the same for the correlation between the IR spectrum and the time of the degradation (see Sect. "[Construction of the hybrid model](#)"). Then, products may be manufactured by any arbitrary processing technique, *e.g.*, injection molding or extrusion. After production, no quality assays that target the analysis of tensile strength are needed. Tensile tests are destructive: at least one product is lost and cannot be sold, *i.e.*, the manufacturer loses money. Moreover, tensile tests assume specific geometry determined by standards, *e.g.*, dumbbell shape. The preparation of such shapes ranges from difficult to impossible in the case of products that have geometries not resembling the shape determined by tensile testing standards.

All these drawbacks can be eliminated by using the method our research group has developed. After the manufacturing of the product, its IR spectrum is to be measured by an ATR accessory. ATR-IR measurements are fast and take only a few minutes, even if the analysis is repeated multiple times. Moreover, the technique is non-destructive, which also means the analyzed product can still be sold. Lastly, ATR-IR measurements do not assume any kind of specific geometry, *i.e.*, no sample preparation is required. Our method only and exclusively needs the measurement of the IR spectrum of the product, preferably multiple times, in order to increase the reliability of the analysis. After pre-processing the averaged spectra, the steps graphically represented in Fig. 10a should be followed. The computation yields an estimated value of the targeted tensile strength. The application of this method is especially beneficial if the parameters of processing are changed during production. Even if the material is degraded to a different extent (*e.g.*, because the residence time has also changed), the model will be able to estimate the tensile strength altered by the modification of the parameters of processing.

Conclusions

Pomegranate extract was found to be an effective stabilizer of PHB. The mechanism of degradation is highly complex, even when there are no additives present in the polymer. The presence of plant extracts in the polymer matrix makes the thorough and complete analysis of all consecutive and parallel reactions that occur during degradation practically impossible. However, the mechanical properties, altered by

the heat shock of processing, can still be predicted. A quick and cost-effective method can be based on simple ATR-IR measurements. Our studies have shown that degradation affects the IR spectrum of PHB considerably. The changes observed on the IR spectra provide a basis for the estimation of the mechanical properties, for example, tensile strength. Such estimation may be based on mathematical models; our results indicated that the most reliable models should consist of at least two parts. The first part describes the nonlinear correlation between the targeted tensile strength and the extent of degradation. In contrast, the second half of the model is linear and is meant to quantitatively characterize the correlation between the extent of degradation and the multidimensional set of IR absorbance values. The combination of the linear and nonlinear parts yields a hybrid model. The concept of this hybrid model was not proposed before: our research group was the first to notice and utilize that linear and nonlinear characteristics can be described simultaneously by combining the partial least squares method with nonlinear regression. This hybrid model was found to be capable of reliably estimating tensile strength despite its limitations, mainly originating from the following factors. First, the model does not take into account that during processing with technologies bearing industrial relevance, mechanical shear inevitably influences the thermo-oxidative degradation of the polymer. Second, the formation of temperature gradients in products is unavoidable, *i.e.*, some regions will cool faster than others. Therefore, the extent of degradation will depend on spatial coordinates. Consequently, the mechanical properties will also vary from location to location, even though the model will provide a prediction only in the region analyzed with ATR-IR. In order to obtain data that can be used safely for prediction, it is recommended to investigate the regions where the process of cooling was the slowest, as the deterioration of mechanical performance is expected to be the most significant there. In spite of all these limitations, the model provides reliable results in the region of degradation times shorter than 8 min. In conclusion, this computational method provides predictions with considerable accuracy in the region bearing practical significance.

Supplementary Information The online version contains supplementary material available at <https://doi.org/10.1007/s10924-023-02934-7>.

Acknowledgements The National Research, Development, and Innovation Fund of Hungary (OTKA PD 138430) is greatly acknowledged for the financial support of this research. This research was also supported by the H2020-MSCA RISE No. 872152—GREEN-MAP project of the European Union and the Polymer Competence Center Leoben GmbH (PCCL, Austria) within the framework of the COMET-program of the Federal Ministry for Transport, Innovation and Technology and Federal Ministry for Economy, Family and Youth.

Author Contributions PP: conceptualization, methodology, resources, writing—original draft, visualization. FM: methodology, investigation,

data curation. ÁT: methodology, investigation. MB: conceptualization, methodology, software, data curation, writing—review & editing.

Funding Open access funding provided by Budapest University of Technology and Economics. All funding bodies are listed in the Acknowledgements section.

Declarations

Competing interest The authors have no relevant financial or non-financial interests to disclose.

Open Access This article is licensed under a Creative Commons Attribution 4.0 International License, which permits use, sharing, adaptation, distribution and reproduction in any medium or format, as long as you give appropriate credit to the original author(s) and the source, provide a link to the Creative Commons licence, and indicate if changes were made. The images or other third party material in this article are included in the article's Creative Commons licence, unless indicated otherwise in a credit line to the material. If material is not included in the article's Creative Commons licence and your intended use is not permitted by statutory regulation or exceeds the permitted use, you will need to obtain permission directly from the copyright holder. To view a copy of this licence, visit <http://creativecommons.org/licenses/by/4.0/>.

References

- Dalsasso RR, Pavan FA, Bordignon SE et al (2019) Polyhydroxybutyrate (PHB) production by *Cupriavidus necator* from sugarcane vinasse and molasses as mixed substrate. *Process Biochem* 85:12–18. <https://doi.org/10.1016/j.procbio.2019.07.007>
- Sen KY, Hussin MH, Baidurah S (2019) Biosynthesis of poly(3-hydroxybutyrate) (PHB) by *Cupriavidus necator* from various pretreated molasses as carbon source. *Biocatal Agric Biotechnol* 17:51–59. <https://doi.org/10.1016/j.bcab.2018.11.006>
- Sakthiselvan P, Madhumathi R (2018) Kinetic evaluation on cell growth and biosynthesis of polyhydroxybutyrate (PHB) by *Bacillus safensis* EBT1 from sugarcane bagasse. *Eng Agric Environ Food* 11:145–152. <https://doi.org/10.1016/j.eaef.2018.03.003>
- García A, Segura D, Espín G et al (2014) High production of poly-β-hydroxybutyrate (PHB) by an *Azotobacter vinelandii* mutant altered in PHB regulation using a fed-batch fermentation process. *Biochem Eng J* 82:117–123. <https://doi.org/10.1016/j.bej.2013.10.020>
- Sharma V, Misra S, Kumar Srivastava A (2017) Developing a green and sustainable process for enhanced PHB production by *Azohydromonas australica*. *Biocatal Agric Biotechnol* 10:122–129. <https://doi.org/10.1016/j.bcab.2017.02.014>
- Poomipuk N, Reungsang A, Plangklang P (2014) Poly-β-hydroxyalkanoates production from cassava starch hydrolysate by *Cupriavidus* sp. KKU38. *Int J Biol Macromol* 65:51–64. <https://doi.org/10.1016/j.ijbiomac.2014.01.002>
- Arumugam A, Senthamizhan SG, Ponnusami V, Sudalai S (2018) Production and optimization of polyhydroxyalkanoates from non-edible *Calophyllum inophyllum* oil using *Cupriavidus necator*. *Int J Biol Macromol* 112:598–607. <https://doi.org/10.1016/j.ijbiomac.2018.02.012>
- Mohidin Batcha AF, Prasad DMR, Khan MR, Abdullah H (2014) Biosynthesis of poly(3-hydroxybutyrate) (PHB) by *Cupriavidus necator* H16 from jatropha oil as carbon source. *Bioprocess Biosyst Eng* 37:943–951. <https://doi.org/10.1007/s00449-013-1066-4>
- Sandhya M, Aravind J, Kanmani P (2013) Production of polyhydroxyalkanoates from *Ralstonia eutropha* using paddy straw as cheap substrate. *Int J Environ Sci Technol* 10:47–54. <https://doi.org/10.1007/s13762-012-0070-6>
- Loan TT, Trang DTQ, Huy PQ et al (2022) A fermentation process for the production of poly(3-hydroxybutyrate) using waste cooking oil or waste fish oil as inexpensive carbon substrate. *Biotechnol Rep* 33:e00700. <https://doi.org/10.1016/j.btre.2022.e00700>
- Muhorakeye A, Cayetano RD, Kumar AN et al (2022) Valorization of pretreated waste activated sludge to organic acids and biopolymer. *Chemosphere* 303:135078. <https://doi.org/10.1016/j.chemosphere.2022.135078>
- Kleidon A (2021) What limits photosynthesis? Identifying the thermodynamic constraints of the terrestrial biosphere within the earth system. *Biochim Biophys Acta BBA* 1862:148303. <https://doi.org/10.1016/j.bbabi.2020.148303>
- Obruca S, Marova I, Snajdar O et al (2010) Production of poly(3-hydroxybutyrate-co-3-hydroxyvalerate) by *Cupriavidus necator* from waste rapeseed oil using propanol as a precursor of 3-hydroxyvalerate. *Biotechnol Lett* 32:1925–1932. <https://doi.org/10.1007/s10529-010-0376-8>
- Abo El-Enin SA, Attia NK, El-Ibiari NN et al (2013) In-situ transesterification of rapeseed and cost indicators for biodiesel production. *Renew Sustain Energy Rev* 18:471–477. <https://doi.org/10.1016/j.rser.2012.10.033>
- Puricelli S, Cardellini G, Casadei S et al (2021) A review on biofuels for light-duty vehicles in Europe. *Renew Sustain Energy Rev* 137:398. <https://doi.org/10.1016/j.rser.2020.110398>
- Drusilla Wendy YB, Nor Fauziah MZ, Siti Baidurah Y et al (2022) Production and characterization of polyhydroxybutyrate (PHB) BY *Burkholderia cepacia* BPT1213 using waste glycerol as carbon source. *Biocatal Agric Biotechnol* 41:102310. <https://doi.org/10.1016/j.bcab.2022.102310>
- Martínez-Herrera RE, Alemán-Huerta ME, Flores-Rodríguez P et al (2021) Utilization of *Agave durangensis* leaves by *Bacillus cereus* 4N for polyhydroxybutyrate (PHB) biosynthesis. *Int J Biol Macromol* 175:199–208. <https://doi.org/10.1016/j.ijbiomac.2021.01.167>
- Polyák P, Szemerszki D, Vörös G, Pukánszky B (2017) Mechanism and kinetics of the hydrolytic degradation of amorphous poly(3-hydroxybutyrate). *Polym Degrad Stab* 140:1–8. <https://doi.org/10.1016/j.polymdegradstab.2017.03.021>
- Polyák P, Dohovits E, Nagy GN et al (2018) Enzymatic degradation of poly-[(R)-3-hydroxybutyrate]: mechanism, kinetics, consequences. *Int J Biol Macromol* 112:156–162. <https://doi.org/10.1016/j.ijbiomac.2018.01.104>
- Polyák P, Urbán E, Nagy GN et al (2019) The role of enzyme adsorption in the enzymatic degradation of an aliphatic polyester. *Enzyme Microb Technol* 120:110–116. <https://doi.org/10.1016/j.enzmictec.2018.10.005>
- Schwarz D, Schoenenwald AKJ, Dörrstein J et al (2018) Biosynthesis of poly-3-hydroxybutyrate from grass silage by a two-stage fermentation process based on an integrated biorefinery concept. *Bioresour Technol* 269:237–245. <https://doi.org/10.1016/j.biortech.2018.08.064>
- Saratale RG, Saratale GD, Cho SK et al (2019) Pretreatment of kenaf (*Hibiscus cannabinus* L.) biomass feedstock for polyhydroxybutyrate (PHB) production and characterization. *Bioresour Technol* 282:75–80. <https://doi.org/10.1016/j.biortech.2019.02.083>
- Tan D, Wang Y, Tong Y, Chen G-Q (2021) Grand Challenges for Industrializing Polyhydroxyalkanoates (PHAs). *Trends Biotechnol* 39:953–963. <https://doi.org/10.1016/j.tibtech.2020.11.010>
- Santos AF, Polese L, Crespi MS, Ribeiro CA (2009) Kinetic model of poly(3-hydroxybutyrate) thermal degradation from

- experimental non-isothermal data. *J Therm Anal Calorim* 96:287–291. <https://doi.org/10.1007/s10973-006-8208-8>
25. Michalak M, Kwiecień M, Kawalec M, Kurcok P (2016) Oxidative degradation of poly(3-hydroxybutyrate). A new method of synthesis for the malic acid copolymers. *RSC Adv* 6:12809–12818. <https://doi.org/10.1039/C5RA27041C>
 26. Zweifel H (1998) Stabilization of polymeric materials. Springer, Berlin
 27. Celina MC (2013) Review of polymer oxidation and its relationship with materials performance and lifetime prediction. *Polym Degrad Stab* 98:2419–2429. <https://doi.org/10.1016/j.polymdegradstab.2013.06.024>
 28. Bredács M, Frank A, Bastero A et al (2018) Accelerated aging of polyethylene pipe grades in aqueous chlorine dioxide at constant concentration. *Polym Degrad Stab* 157:80–89. <https://doi.org/10.1016/j.polymdegradstab.2018.09.019>
 29. Ambrogi V, Cerruti P, Carfagna C et al (2011) Natural antioxidants for polypropylene stabilization. *Polym Degrad Stab* 96:2152–2158. <https://doi.org/10.1016/j.polymdegradstab.2011.09.015>
 30. Mayer J, Metzsch-Zilligen E, Pfaendner R (2022) Novel multifunctional antioxidants for polymers using eugenol as biogenic building block. *Polym Degrad Stab* 200:109954. <https://doi.org/10.1016/j.polymdegradstab.2022.109954>
 31. Abdul Khalil HPS, Lai TK, Tye YY et al (2018) A review of extractions of seaweed hydrocolloids: properties and applications. *Express Polym Lett* 12:296–317. <https://doi.org/10.3144/expresspolymlett.2018.27>
 32. Nanni A, Battezzore D, Frache A, Messori M (2019) Thermal and UV aging of polypropylene stabilized by wine seeds wastes and their extracts. *Polym Degrad Stab* 165:49–59. <https://doi.org/10.1016/j.polymdegradstab.2019.04.020>
 33. Battezzore D, Bocchini S, Alongi J, Frache A (2014) Plasticizers, antioxidants and reinforcement fillers from hazelnut skin and cocoa by-products: extraction and use in PLA and pp. *Polym Degrad Stab* 108:297–306. <https://doi.org/10.1016/j.polymdegradstab.2014.03.003>
 34. Rasselet D, Ruellan A, Guinault A et al (2014) Oxidative degradation of polylactide (PLA) and its effects on physical and mechanical properties. *Eur Polym J* 50:109–116. <https://doi.org/10.1016/j.eurpolymj.2013.10.011>
 35. Gardette M, Thérias S, Gardette J-L et al (2011) Photooxidation of polylactide/calcium sulphate composites. *Polym Degrad Stab* 96:616–623. <https://doi.org/10.1016/j.polymdegradstab.2010.12.023>
 36. Keithley RB, Mark Wightman R, Heien ML (2009) Multivariate concentration determination using principal component regression with residual analysis. *TrAC Trends Anal Chem* 28:1127–1136. <https://doi.org/10.1016/j.trac.2009.07.002>
 37. Mehmood T, Liland KH, Snipen L, Sæbø S (2012) A review of variable selection methods in partial least squares regression. *Chemom Intell Lab Syst* 118:62–69. <https://doi.org/10.1016/j.chemolab.2012.07.010>
 38. Schmidt J, Gergely S, Schönlechner R et al (2009) Comparison of different types of NIR instruments in ability to measure β -glucan content in naked barley. *Cereal Chem J* 86:398–404. <https://doi.org/10.1094/CCHEM-86-4-0398>
 39. Hódsági M, Gergely S, Gelencsér T, Salgó A (2012) Investigations of native and resistant starches and their mixtures using near-infrared spectroscopy. *Food Bioprocess Technol* 5:401–407. <https://doi.org/10.1007/s11947-010-0491-5>
 40. Kozma B, Hirsch E, Gergely S et al (2017) On-line prediction of the glucose concentration of CHO cell cultivations by NIR and Raman spectroscopy: comparative scalability test with a shake flask model system. *J Pharm Biomed Anal* 145:346–355. <https://doi.org/10.1016/j.jpba.2017.06.070>
 41. Lin C, Chen X, Jian L et al (2014) Determination of grain protein content by near-infrared spectrometry and multivariate calibration in barley. *Food Chem* 162:10–15. <https://doi.org/10.1016/j.foodchem.2014.04.056>
 42. Long DS, Engel RE, Siemens MC (2008) Measuring grain protein concentration with in-line near infrared reflectance spectroscopy. *Agron J* 100:247–252. <https://doi.org/10.2134/agronj2007.0052>
 43. Xu F, Corbett B, Bell S et al (2020) High-throughput synthesis, analysis, and optimization of injectable hydrogels for protein delivery. *Biomacromolecules* 21:214–229. <https://doi.org/10.1021/acs.biomac.9b01132>
 44. Bredács M, Barretta C, Castillon LF et al (2021) Prediction of polyethylene density from FTIR and Raman spectroscopy using multivariate data analysis. *Polym Test* 104:107406. <https://doi.org/10.1016/j.polymertesting.2021.107406>
 45. Ambigaipalan P, de Camargo AC, Shahidi F (2016) Phenolic compounds of pomegranate byproducts (outer skin, mesocarp, divider membrane) and their antioxidant activities. *J Agric Food Chem* 64:6584–6604. <https://doi.org/10.1021/acs.jafc.6b02950>
 46. Fischer UA, Carle R, Kammerer DR (2011) Identification and quantification of phenolic compounds from pomegranate (*Punica granatum* L.) peel, mesocarp, aril and differently produced juices by HPLC-DAD-ESI/MSn. *Food Chem* 127:807–821. <https://doi.org/10.1016/j.foodchem.2010.12.156>
 47. Tátraaljai D, Tang Y, PREGI E et al (2022) Stabilization of PE with pomegranate extract: contradictions and possible mechanisms. *Antioxidants* 11:418. <https://doi.org/10.3390/antiox11020418>
 48. Oudane B, Boudemagh D, Bounekhel M et al (2018) Isolation, characterization, antioxidant activity, and protein-precipitating capacity of the hydrolyzable tannin punicalagin from pomegranate yellow peel (*Punica granatum*). *J Mol Struct* 1156:390–396. <https://doi.org/10.1016/j.molstruc.2017.11.129>
 49. Feng L, Yin Y, Fang Y, Yang X (2017) Quantitative determination of punicalagin and related substances in different parts of pomegranate. *Food Anal Methods* 10:3600–3606. <https://doi.org/10.1007/s12161-017-0916-0>
 50. Mark H, Workman J (2018) Chemometrics in spectroscopy. Elsevier, Amsterdam
 51. de Jong S (1993) SIMPLS: an alternative approach to partial least squares regression. *Chemom Intell Lab Syst* 18:251–263. [https://doi.org/10.1016/0169-7439\(93\)85002-X](https://doi.org/10.1016/0169-7439(93)85002-X)
 52. Roman L, Campanella O, Martinez MM (2019) Shear-induced molecular fragmentation decreases the bioaccessibility of fully gelatinized starch and its gelling capacity. *Carbohydr Polym* 215:198–206. <https://doi.org/10.1016/j.carbpol.2019.03.076>
 53. Domenek S, Berzin F, Ducruet V et al (2021) Extrusion and injection moulding induced degradation of date palm fibre - polypropylene composites. *Polym Degrad Stab* 190:9641. <https://doi.org/10.1016/j.polymdegradstab.2021.109641>
 54. Lladó J, Sánchez B (2008) Influence of injection parameters on the formation of blush in injection moulding of PVC. *J Mater Process Technol* 204:1–7. <https://doi.org/10.1016/j.jmatprotec.2007.12.063>

Publisher's Note Springer Nature remains neutral with regard to jurisdictional claims in published maps and institutional affiliations.